Assessing effects of native forest restoration on soil moisture dynamics and potential aquifer recharge, Auwahi, Maui

Kim S. Perkins,[1]* John R. Nimmo,[1] Arthur C. Medeiros,[2] Daphne J. Szutu[1] and Erica von Allmen[2]

[1] *U.S. Geological Survey, 345 Middlefield Rd., MS-421, Menlo Park, California, 95119, USA*
[2] *U.S. Geological Survey, Pacific Island Ecosystems Research Center, Haleakalā National Park Field Station, P.O. Box 369, Makawao, Hawai'i, 96768, USA*

ABSTRACT

Understanding the role of soils in regulating water flow through the unsaturated zone is critical in assessing the influence of vegetation on soil moisture dynamics and aquifer recharge. Because of fire, introduced ungulates and landscape-level invasion of non-native grasses, less than 10% of original dry forest (~730 mm precipitation annually) still exists on leeward Haleakalā, Maui, Hawaiian Islands. Native dry forest restoration at Auwahi has demonstrated the potential for dramatic revegetation, allowing a unique experimental comparison of hydrologic function between tracts of restored forest and adjacent grasslands. We hypothesized that even relatively recent forest restoration can assist in the recovery of impaired hydrologic function, potentially increasing aquifer recharge. To compare restored forest and grassland sites, we experimentally irrigated and measured soil moisture and temperature with subsurface instrumentation at four locations within the reforested area and four within the grassland, each with a 2·5 × 2·5-m plot. Compared with grassland areas, water in reforested sites moved to depth faster with larger magnitude changes in water content. The median first arrival velocity of water was greater by a factor of about 13 in the reforested sites compared with the grassland sites. This rapid transport of water to depths of 1 m or greater suggests increased potential aquifer recharge. Improved characterization of how vegetation and soils influence recharge is crucial for understanding the long-term impacts of forest restoration on aquifer recharge and water resources, especially in moisture-limited regions. Published 2014. This article is a U.S. Government work and is in the public domain in the USA.

KEY WORDS   infiltration; preferential flow; reforestation; unsaturated zone; aquifer recharge; soil moisture

Received 27 March 2013; Revised 20 December 2013; Accepted 20 December 2013

INTRODUCTION

Many studies have shown that land use directly affects ecohydrology (Grayson *et al.*, 2006; Sandvig and Phillips, 2006; D'Odorico *et al.*, 2007; Nimmo *et al.*, 2009; Brauman *et al.*, 2012a, 2012b) and specifically soil hydraulic properties (Godsey and Elsenbeer, 2002; Zimmermann and Elsenbeer, 2008; Berglund *et al.*, 1980; Wahren *et al.*, 2009). Human alteration of landscapes such as deforestation, introduction of invasive species, agriculture, and urban development has significantly altered ecosystems globally. Biologically, these disturbances have resulted in habitat loss, degradation, and species extinction. Disruption of fundamental interrelationships between ecologic, hydrologic, and geologic processes can cause significant changes to ecosystem structure and function. Impacts to the unsaturated zone include alteration of soil hydraulic properties and processes, water quality and availability, rainfall/run-off partitioning, erosion, habitat suitability, biodiversity, and ecological health and change.

In the Hawaiian archipelago, dry forest ecosystems have high plant species diversity but are fragmented, reduced, and ecologically degraded, with less than 10% remaining (Medeiros *et al.*, 1986; Cabin *et al.*, 2001, Medeiros *et al.*, 2013). The impacts of introduced grazing ungulates, fire, and invasive species have resulted in replacement of much of the original dry forest with non-native grasslands (Cabin *et al.*, 2001). Relictual Hawaiian dry forests are not only the last sanctuary for many rare Hawaiian species (Rock, 1913) including over 25% of federally-listed endangered Hawaiian plant species (Cabin *et al.*, 2001), but also species with great importance to the Hawaiian culture (Medeiros *et al.*, 1998).

Several studies in Hawai'i have demonstrated the effects of the loss of native forests on the near-surface hydrology (Stock *et al.*, 2003; Scholl *et al.*, 2007), as well as the capability of native vegetation to increase water inputs to soil (Giambelluca *et al.*, 2011b). However, until this study, the role of soil hydraulic properties and subsurface moisture dynamics as influenced by vegetation has not been fully investigated by using direct field measurements. A preliminary study conducted in 2011 demonstrated that over 14 years, reintroduced native plants at the Auwahi site on Maui (Figure 1) have significantly altered shallow soil hydraulic

*Correspondence to: U.S. Geological Survey, 345 Middlefield Rd., MS-421, Menlo Park, California, 95119, USA.
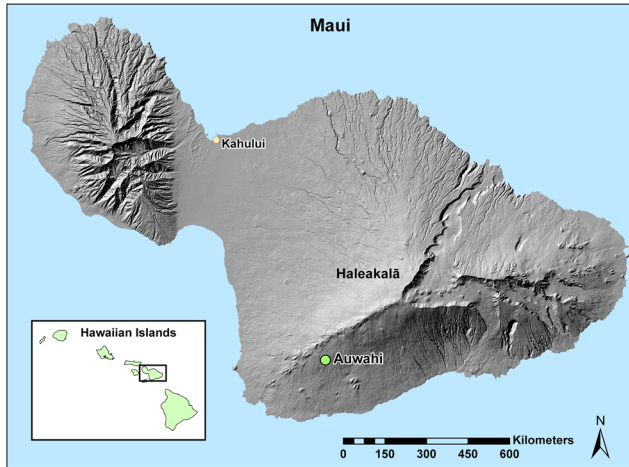E-mail: kperkins@usgs.gov

Figure 1. Map of Maui and location of the Auwahi site, on the leeward side of Haleakalā.

properties (Perkins *et al.*, 2012). Compared with analogous locations in nearby deforested grassland, the restored forest had a mean field-saturated hydraulic conductivity (K_{fs}) 49% greater as measured by 54 infiltrometer tests. Surface hydrophobicity increased from very strongly to extremely hydrophobic. A 4-point empirical categorization of preferentiality in subsurface wetting patterns increased from an average of 1·3 to 2·6 when comparing forest and grassland areas. Each result is significant at the level of 95% or greater.

Hydrophobicity, hydraulic conductivity, and preferential flow are inherently linked properties. Zhou *et al.* (2008) found that forest soils tend to have higher K_{fs} because they generally have higher organic matter content leading to aggregate stability and increased number of macropores. Increased organic matter and resulting hydrophobicity have been found to induce unstable or fingered flow, enhancing vertical flow (Hardie *et al.*, 2012; Xiong *et al.*, 2012). Bachmair *et al.* (2009) found that even though their study sites had similar soil texture and the same parent material, land cover made a difference in preferential flow processes because of different soil structure among sites (e.g. macropores). Similarly, Alaoui *et al.* (2011) found that grassland sites have less efficient macropores than forested sites with increased soil moisture at forested sites. Few field sites provide the venue necessary to do rigorous, comparative studies on which changes can be evaluated over different land use areas. A meta-analysis study on the effect of forested vegetation cover on infiltration (Ilstedt *et al.*, 2007) found that most published studies were not sufficiently robust in terms of experimental design to determine significant differences.

To compare hydrologic responses between tracts of newly restored (ca 15 year) native forest and adjacent invasive grasslands at Auwahi, we simulated a large magnitude rainfall storm event by experimentally irrigating and measuring soil moisture and temperature at multiple locations and variable depths with subsurface instrumentation. The primary
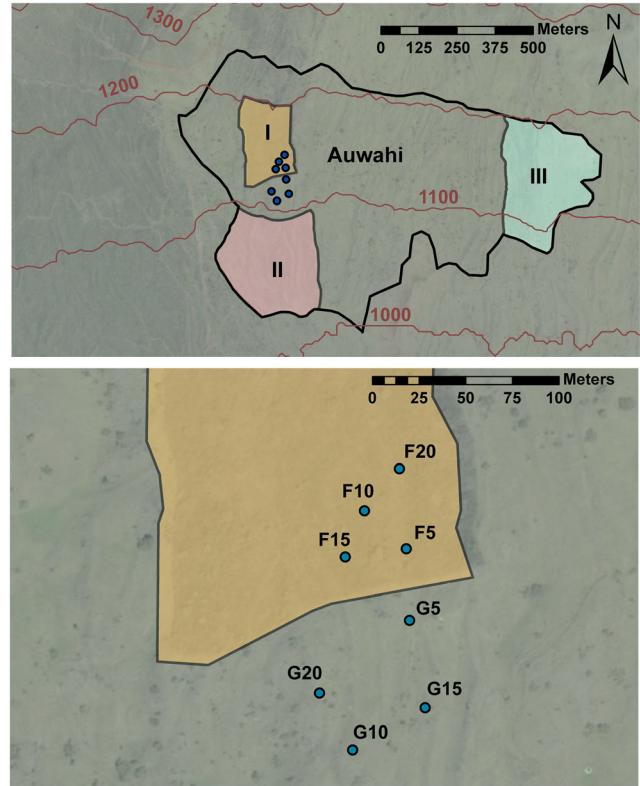

Figure 2. Map of Auwahi site with locations of sprinkling irrigation experiments. Forest plots (F5, F10, F15, and F20) are located within Auwahi I, and Grassland plots (G5, G10, G15, and G20) are located south of Auwahi I.

questions of this investigation are the following: (1) does water move differently through the soil at the forest and grassland sites? and (2) does water infiltrate deep enough to become potential recharge to regional aquifers?

METHODS

Site description

Forest restoration efforts at Auwahi (Figure 1), on the leeward slope of Haleakalā, Maui, began in 1997 with a 4-ha tract (Auwahi I, Figures 2 and 3) between 1100- and 1200-m elevation that was fenced to exclude grazing ungulates (Medeiros *et al.*, 2003). Mats of invasive kikuyu grass (*Cenchrus* (*Pennisetum*) *clandestinus*) were treated with herbicides, and the restoration area was replanted with native tree, shrub, vine, and grass species, including five endangered species, that were elements of the original community (Medeiros *et al.* 1986; Medeiros and von Allmen, 2006; Medeiros *et al.*, 2013). The ongoing restoration effort now includes three fenced tracts totalling almost 18 ha (Figure 2). At Auwahi, restoration has increased shrub-tree cover from 8·6% to 68·0% and reduced cover of non-native grasses from 70·9% to 0·3% (Medeiros *et al.*, 2013). Unassisted natural seedling recruitment is now common within the reestablished native forest (Medeiros *et al.*, 2013).

Figure 3. Overhead view of Auwahi I exclosure.

The site has relatively thin (a few centimetre to about 1 m), stoney soils with outcrops of basalt rubble that form ridges across the landscape. Soils are the only likely impediment to rapid flow through the highly permeable rock. The soils in the vicinity of Auwahi are classified as andisols in the Ulupalakua Series with weak development and sandy texture. The type taxonomic class is medial over pumiceous or cindery, amorphic, isothermic Pachic Haplustand (USDA, 2001). Because of the rugged nature of the surface terrain, rocky subsurface, and limited accessibility (fencing around the forest prohibits vehicle access), soil profiles were examined not in pits at the site of experiments but in nearby road cut exposures vegetated with mainly invasive and sparse native species (more comparable with the grass plots than the forest). Because the forest was planted recently (~15 years ago), it is likely that the dominant soil forming processes would be due to changing root structure. The following soil descriptions rely on the U.S. Department of Agriculture Soil Survey Manual (USDA, 1993). The soil is described in Table I. The Auwahi soils are very stoney throughout with diffuse, wavy horizon boundaries; therefore, horizon boundaries are approximate (Figure 4). There is a thick organic mat of grass above the soil surface, an organic-rich A horizon from 0–20-cm depth, a B1 horizon from 20–40 cm that is lighter in colour with less organic matter incorporation, a B2 horizon from 40–80 cm that is slightly finer in texture (11% sand and silt compared with 7–8% above), and a C horizon below 80-cm depth. Soil samples were collected for particle-size analysis from 0–20 cm, 20–40 cm, 40–60 cm (Figure 4). The soil exposures provide evidence of the variability of soil depth across the landscape. Slopes are moderately steep to steep. Ground surface cover was estimated for the eight plots. The grass plots were all 100% covered in live vegetation; details for the forest plots are given in Table II.

The site receives 730 mm of precipitation annually (Giambelluca *et al*., 2011a). Outside of the rift zones,

Table I. Description of the soil profile at a road cut adjacent to the experimental site.

| Horizon	Depth interval (cm)	Horizon boundary	Structure	Texture	Colour (dry)	Consistence (dry: moist)	Roots
A	0–20	Diffuse, wavy	Fine-medium granular	Cobbly sand	Black, 10YR 2/1	slightly hard: very friable	many very fine to medium
B1	20–40	Diffuse, wavy	Fine-medium granular	Very cobbly sand	Very dark brown, 10YR 3/2	slightly hard: very friable	many very fine to medium
B2	40–80	Diffuse, wavy	Fine-medium granular	Very cobbly sand	Very dark brown, 10YR 3/2	slightly hard: very friable	many very fine to medium
C	>80	Gradual, wavy	n/a	n/a	n/a	n/a	n/a
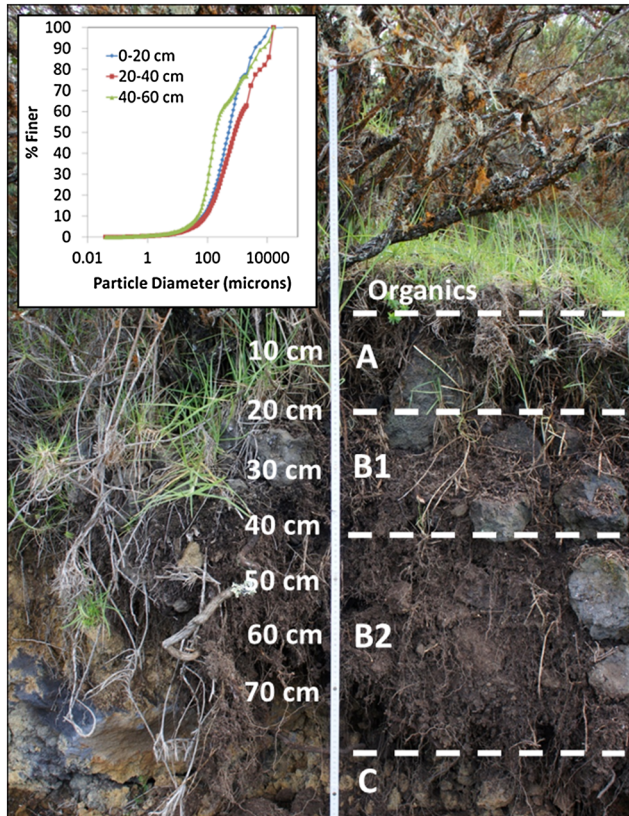
Figure 4. Soil profile photo with horizons marked by horizontal vertical line and particle size distributions of Horizons A (0–20-cm depth), B1 (20–40-cm depth), and B2 (40–60-cm depth).

Table II. Soil surface charateristics of the four forest sites.

Site	Exposed rock (%)	Bare soil (%)	Leaf litter (%)	Dominant species
F1	15	5	80	ʻaʻaliʻi
F2	30	5	65	ʻaʻaliʻi
F3	30	0	70	olopua
F4	20	10	70	ʻaʻaliʻi

groundwater levels on the island of Maui are generally only about a metre above sea level in leeward Haleakala (Gingerich, 2008)). Thus, the depth to the aquifer can be approximated (within about 1 m) by the land surface altitude.

Field methods

The findings of increased K_{fs}, hydrophobicity, and preferential flow in the reforested area at Auwahi (Perkins *et al.*, 2012) prompted additional, more extensive field experiments to examine deeper soil moisture dynamics as a result of artificial and naturally occurring, storm-sized infiltration events. We conducted an infiltration and monitoring study to assess soil moisture dynamics in the unsaturated zone to gain insight into recharge processes beneath the

restored Auwahi native forest [with dominant species being *olopua* trees (*Nestegis sandwicensis*) and ʻaʻaliʻi shrubs (*Dodonaea viscosa*)] and adjacent invasive grassland [dominated by kikuyu grass (*C. clandestinus*)].

By using water application by drip irrigation tubing to simulate rainfall, we conducted separate infiltration tests on eight plots, 2·5 × 2·5 m each, in September 2012; four were in the restored forest and four in the grassland. The plots were chosen based on accessibility within the rugged landscape and soil thickness, with thick soils being desirable for observing deep water movement. A total of 160, soil moisture and temperature sensors were installed to monitor soil moisture profile dynamics at these eight plots. The plots are named according to the vegetation (F prefix for forest and G prefix for grassland) and amount of irrigation received (5, 10, 15, and 20 cm). The eight plots are hereafter referred to as F5, F10, F15, F20, G5, G10, G15, and G20. A combination of soil moisture sensors were used: Enviroscan moisture profiling probes (Sentek Technologies[†]) with sensors every 10 cm down to 1 m and Decagon[1] EC-5 probes, each with a single sensor, installed at 2–3-cm depths at each plot (see Table III for depth of sensors at each plot). The probes were not calibrated to the native soil; therefore, we used the manufacturer calibration. EC-5 probes were installed in holes augered diagonally and backfilled with a mixture of native soil, kaolinite, and bentonite packed tightly to prevent creation of preferential flow paths. Two Enviroscan probes (one in the forest and one in the grassland) had annular gaps in their installation holes, potentially causing artificial preferential flow and hence requiring kaolinite slurry backfilling as recommended by the manufacturer. Custom-built temperature rods with thermistors at 20-, 40-, 60-, 80-, 90-, and 100-cm depths plot (see Table III for depth of sensors at each plot) were also installed to provide proxy data for water content change (Stewart-Deaker *et al.*, 2007). Figure 5 shows example subsurface instrumentation maps in cross section and plan view. Instruments were installed down to 1-m depth, or as close to it as physically possible, the intention being to have one or more sensors deep enough that the water may be less vulnerable to evapotranspiration and therefore potentially available to become recharge.

Water was supplied by gravity feed from a 7600-L tank upslope from the field site, flow equalized with inline pressure regulators, and delivered by drip irrigation tubing spaced approximately every 20 cm over the plots with emitters every 20 cm (Figure 6). Four treatments were applied at a constant rate of 25 mm h^{-1} on 18 September 2012 to both forest and grassland sites to simulate 5, 10, 15, or 20 cm precipitation events (Table III). The following day, the experiments were repeated at all eight plots . However, the 2 plots previously receiving 20 cm only received 15 cm due to time constraints.

[†]Mention of brand names does not constitute endorsement by the US Geological Survey

Ecohydrol. (2014)

Table III. Plot treatment and depth of water content and temperature sensors installed.

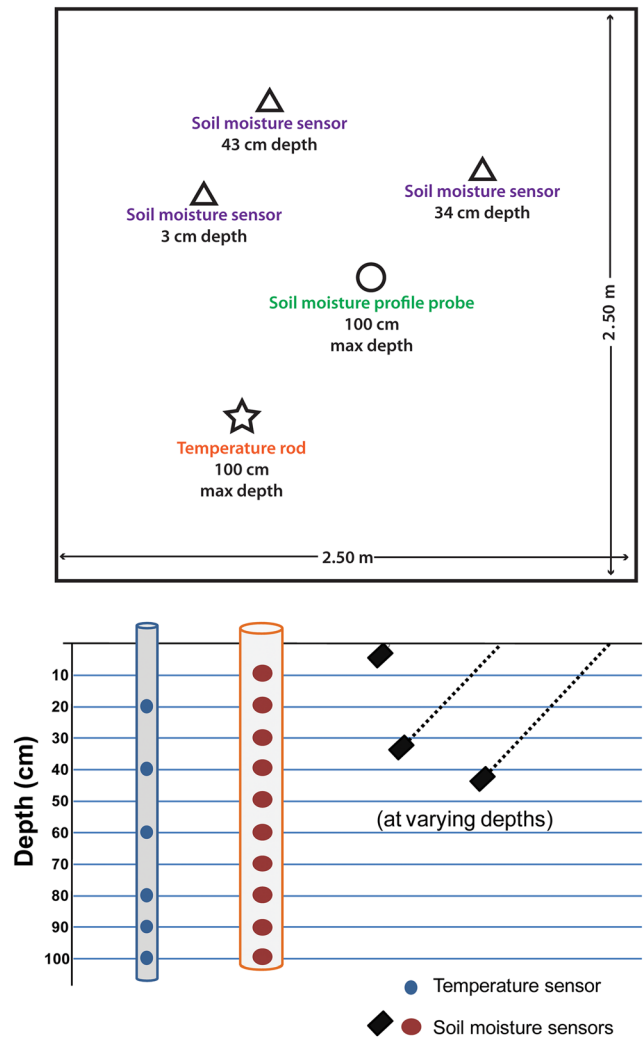| | | Plot | | | | | | | |
		F5	F10	F15	F20	G5	G10	G15	G20
Treatment on 18 September 2012 (cm) 'dry application'		5·1	10·2	15·2	20·3	5·1	10·2	15·2	20·3
Treatment on 19 September 2012 (cm) 'wet application'		5·1	10·2	15·2	15·2	5·1	10·2	15·2	15·2
Probe									
Enviroscan water content probes	Sensor depth range (cm)	10–100	5–75	1–90	10–100	5–65	3–63	6–96	8–78
	Offset from legend (cm, Figure 6)	0	−5	−10	0	−5	−7	−4	−2
EC–5 water content sensors	Sensor depths (cm)	3, 66	3, 24, 42	3, 24, 42	3, 55	3, 24, 42	3, 40	3, 34, 42	3, 48
Temperature probes	Sensor depth range (cm)	20–100	20–100	20–100	20–100	8–88	33–73	20–100	20–100
	Offset from legend (cm, Figure 7)	0	0	0	0	−12	+13	0	0

Figure 5. Map view (top) and cross section (bottom) of a typical plot layout. Instrumentation includes: temperature rod with six sensors to 1-m depth, soil moisture profile probe with 10 sensors to 1-m depth, and the 2–3 soil moisture sensors at various depths at each plot.

Each location was hand regulated with valves and a flow metre to ensure that the correct volume was applied at each site.

Hydrophobicity measurements were taken at the soil surface and at 25-cm depth near each of the eight plots by using molarity of ethanol droplet tests as implemented by Doerr (1998). The test uses an 8-point scale and is designed to use the rapidity of infiltration of droplets of water with varying ethanol concentrations as a metric for hydrophobicity. Solutions were mixed with ethanol concentrations of 0, 3, 5, 8·5, 13, 24, and 36% by volume diluted with deionized water. Time for droplet penetration was measured and soils were rated accordingly. The rating corresponds to the highest concentration of droplet that penetrated the soil in under 3 s. The eighth point of the scale is implicit as the possibility that for soils at the highest extremes of hydrophobicity the 36-percent solution may not penetrate in less than 3 s.

Figure 6. Photo of typical 2·5 × 2·5 m plots in the grassland and forest, showing irrigation tubing used for infiltration experiment.

Laboratory methods

A Coulter LS-230 Particle Size Analyzer was used to characterize particle-size distributions by optical diffraction (Gee and Or, 2002). The range of measurement for this device is 0·04–2000 μm, which is divided into 116-μm size bins. Any particles greater than 2000 μm were sieved out and later integrated into the particle-size distribution results. The fraction less than 2000 μm was disaggregated carefully using a mortar and rubber-tipped pestle, and then split with a 16-compartment spinning riffler to obtain appropriate random samples for analysis. The material was sonicated in suspension for 60 s prior to each run; an average of two runs was calculated for each sample.

Data analysis methods

The water content data allowed us to assess water velocity, magnitude of water content changes, and differences in soil water dynamics because of the amount of water added. The temperature data were utilized primarily to determine first arrival of applied water as the irrigated input water temperature begins to equilibrate with the soil water over time.

We calculated the first arrival velocity using data from both water content sensors and temperature sensors. The time of first arrival was determined manually and defined as the minute that the water content or temperature sensor showed a monotonic increase from the baseline of at least 0·002 in volumetric water content or 0·125 °C in temperature. The baseline water content and temperature at each location and each sensor were observed from the 2- or 3-day equilibration period after probes were installed and before sprinkling began. The first arrival velocity was calculated by dividing the depth of the sensor by the time of first arrival at that sensor. First arrival velocity data were grouped into four depth intervals: 0–24, 25–49, 50–74, and 75–100 cm.

For analysing the magnitude of water content change, because only water content sensor data could be used and large enough population counts were needed for valid statistical analysis, data were grouped into depth intervals of 0–49 and 50–100 cm instead of the four depth intervals used for the first arrival velocity analysis. The magnitude of water content increase was calculated by subtracting baseline water content from the maximum water content recorded. The maximum recorded water content usually coincided with the end of irrigation, but in a few cases it occurred as much as 2 h earlier (G20, sensor at 40-cm depth) or 5 h later (G10, sensor at 63-cm depth). The magnitude of water content decrease observed after the infiltration events was calculated by subtracting the water content 12 h after irrigation ceased from the maximum water content recorded for each event. For example, irrigation on 18 September 2012 at location F5 ended at 1043 h; to calculate the magnitude of water content decrease, the water content at 2243 h at each sensor was subtracted from the water content at 1043 h at each sensor.

Cumulative increase water content data were analysed using data from plots F5, F20, G5, G10, G15, and G20 as these plots had water content data from both 18 and 19 September 2012. These data were divided into four groups to produce an average value for depths 0–49 cm in the forest, 50–100 cm in the forest, 0–49 cm in the grassland, and 50–100 cm in the grassland. For example, data from all water content sensors 0–49 cm in the two forest plots (five sensors total) were averaged at each minute to create a single value at each time step for the increase in average water content data for depths 0–49 cm in the forest. The cumulative increase was calculated from a baseline water content of 17 September 2012, at 1205 h for the forest plots and at 1530 h for the grassland plots. At each time step, we calculated the cumulative increase by adding the increase in average water content increase from the previous time step, or 0, whichever was bigger. Similarly, at each time step, we calculated the cumulative decrease by subtracting the decrease in average water content from the previous time step, or 0, whichever was smaller.

For statistical analyses, normality of distributions of water content change and first arrival velocity data were tested using normal quantile plots. To assess the significance of differences in measured data between depths or locations, we used the Wilcoxon rank sum test, also known as the Mann–Whitney test (Zar, 1999), because of nonnormality of our data. This test is a non-parametric analogue to a two-sample *t*-test for establishing differences between two distributions. The test ranks the values of the combined distributions and calculates the sum of the ranks

(the rank sum) from each distribution. If the rank sum of the distribution is far from the mean rank sum (calculated assuming the two distributions are random), the test rejects the null hypothesis that the distributions are the same.

RESULTS

As indicated by both water content and temperature data, the probes showed distinct subsurface responses to infiltrate water. Figure 7 gives the time series of measured water contents for the experiments on both days. Figure 8 gives the time series of measured temperatures on the first day. The temperature data indicate the presence of newly infiltrated water because the water applied was warmer than antecedent soil temperatures. There was no observed run-off at any of the plots.

The data collectively show that subsurface arrival times and the slope, smoothness, and magnitude of change varied greatly between and within the forest and grassland plots. Noteworthy observations of wetting behaviour and comparison of all plots are given in Table IV. Many sensors indicated strong and rapid increases in wetness. Most plots had out-of-sequence water content changes (i.e. responses at a given depth interval before those of overlying intervals). Some plots showed much larger responses at deeper depths than shallower. These effects indicate a strong influence of preferential flow. During the infiltration interval, some plots, notably G10, show oscillations with a period of about 10 min, likely resulting from irrigation valve operations. The temperature data also showed flow behaviour variability and distinct differences that qualitatively confirm the behaviour of infiltrated water also indicated by the water content sensors.

Major qualitative features of the data sets show no significant dependence on the amount or duration of infiltration, even though the amount added to different plots differed by as much as a factor of four. The amount of water added had no significant influence on the first arrival velocity (Figure 9). Observations to 1-m depth in both forest and grassland showed no apparent relationship between maximum depth reached by infiltrated water and the amount of water applied; in all cases, water infiltrated to the deepest sensors. In a similar comparative study, Bachmair *et al.* (2009) also found no correlation of irrigation treatment and maximum depth reached by infiltration. These observations relate to the fact that most of the water content changes take place quickly; therefore, longer sprinkling times had no apparent effect on these responses.

Water velocities from both water content and temperature sensors indicate rapid movement through the upper 50 cm of soil in both forest and grassland (Table V and Figure 10). From 25- to 100-cm depth, at the 95% confidence level or higher, average first arrival velocities

were faster at reforested plots. At depths below 75 cm, this effect was very pronounced, with the median first arrival velocity greater by a factor of about 13 in the reforested plots compared with the grassland plots and statistically different at the 99% confidence level. In summary, in the grassland plots, water movement slowed with depth; whereas at the reforested plots, rapid water movement occurred through the entire upper metre of the soil.

Some water content sensors, for example at F20 and G10, show fairly rapid declines in water content at cessation of infiltration. For others, as at F5 and G20, the decline is gradual or indistinguishable over the measurement period. Where the decline is initially rapid, after a time of less than about 30 min, the rate of decline slows markedly although the water content is still well above the pre-infiltration water content. These results suggest that most water that has arrived at depth is held in place by capillarity, though some may move elsewhere by preferential flow.

Some of the Enviroscan sensors at plots F10, F20, G10, G15, and G20 indicate essentially zero water content over the period of measurement. The likely cause is a near-absence of water within the volume to which the sensor is sensitive. A sensor will read essentially zero when the material within that volume has a very low dielectric constant, like that of air or rock. Given the extremely stony soil in which the probes were installed, it is possible that some of the volumes of sensitivity were occupied by air or rubbly material without enough fine particles to retain significant water. These data were excluded in the analysis as there was no measurable change in water content.

Data from EC-5 sensors are useful from all plots. Data from Enviroscan probes are useful from all plots except F15 and G5, where the slurry used to fill annular space in the installation affected those water content measurements much more than expected. Those two probes indicated a magnitude of water content change much less than the actual change, possibly because the slurry did not have sufficient time to dry or because Kaolinite may be less sensitive to water content change. Data from the shallowest (5 cm) sensor at G5, however, appears less affected by the slurry, as judged from the pattern of response (arrival time, magnitude, slope, and smoothness), which is similar to that of the 3 cm EC-5 sensors at G5. The probe at G20 was similarly backfilled with bentonite near the surface, and its uppermost sensor did not produce useful water content data. As the sensors were not calibrated to the native soils, the data indicate relative changes in water content but not absolute water content.

Owing to the slowness of the long-term decline in wetness, the initial water contents on the second day of experiments were higher (where nonzero) than on the first day. However, comparison of the 2 days does not show major qualitative differences in behaviour.

Figure 11 shows the cumulative record of water content increases averaged from all probes exclusive of decreases for
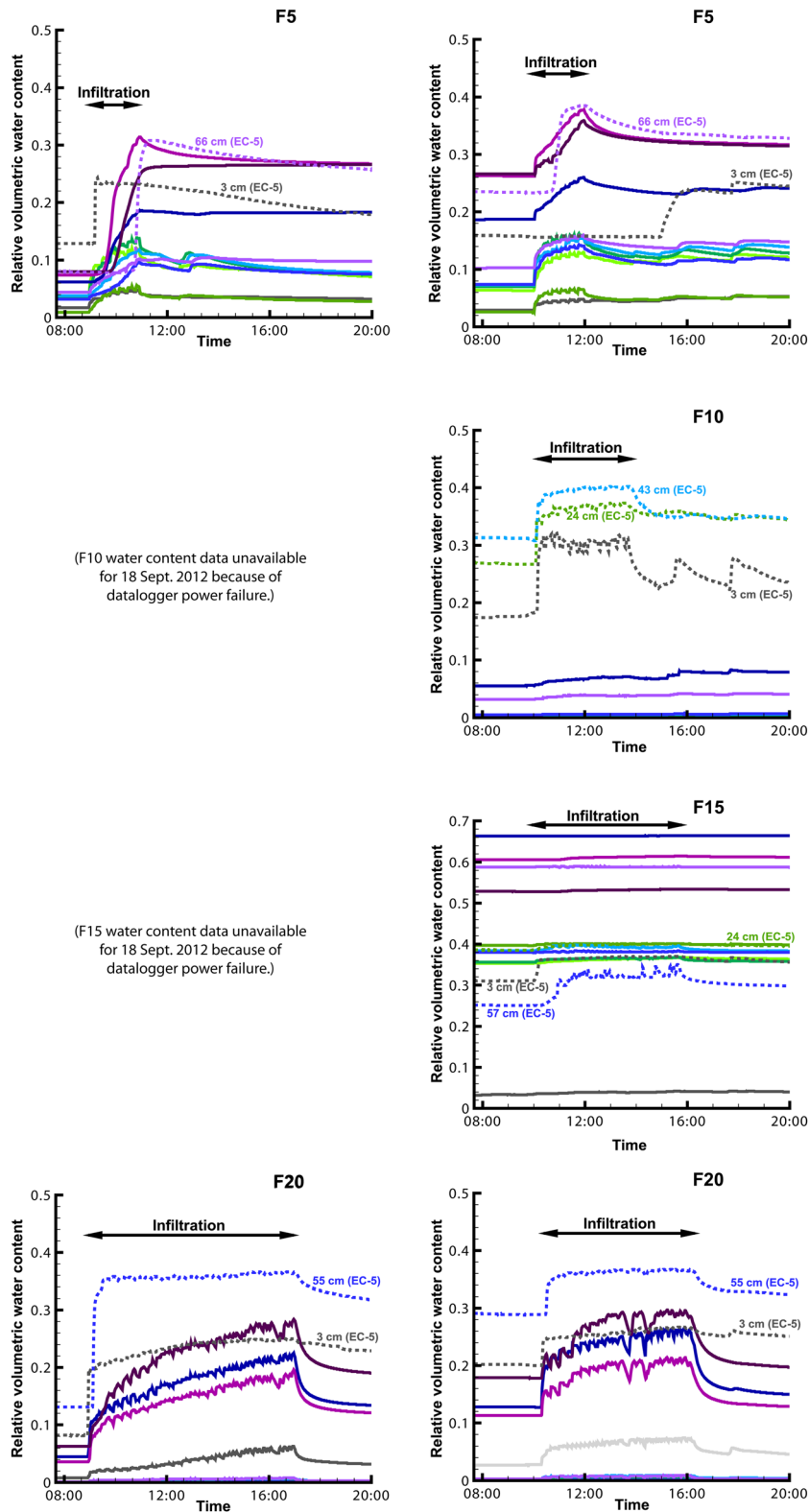
Figure 7. Response to the 18 September 2012 ('dry' application, left column) and 19 September 2012 ('wet' application, right column) artificial infiltration event of water content sensors. Graphs are ordered in increasing magnitude of treatment (5·1 cm at the top to 20·3 cm at the bottom). Response at different depths is indicated by different-coloured lines. Solid lines indicate Sentek EnviroSCAN sensors and dashed lines indicate Decagon EC-5 sensors. Enviroscan water content sensors were installed at 10–100-cm depth, as indicated in the legend. Sites F10, F15, G5, G10, G15, and G20 have sensor depths that are offset from the legend (Table III). Note that the absolute value differences between the probe typess is because of factory calibration. The period of infiltration at each plot is marked with a horizontal line.
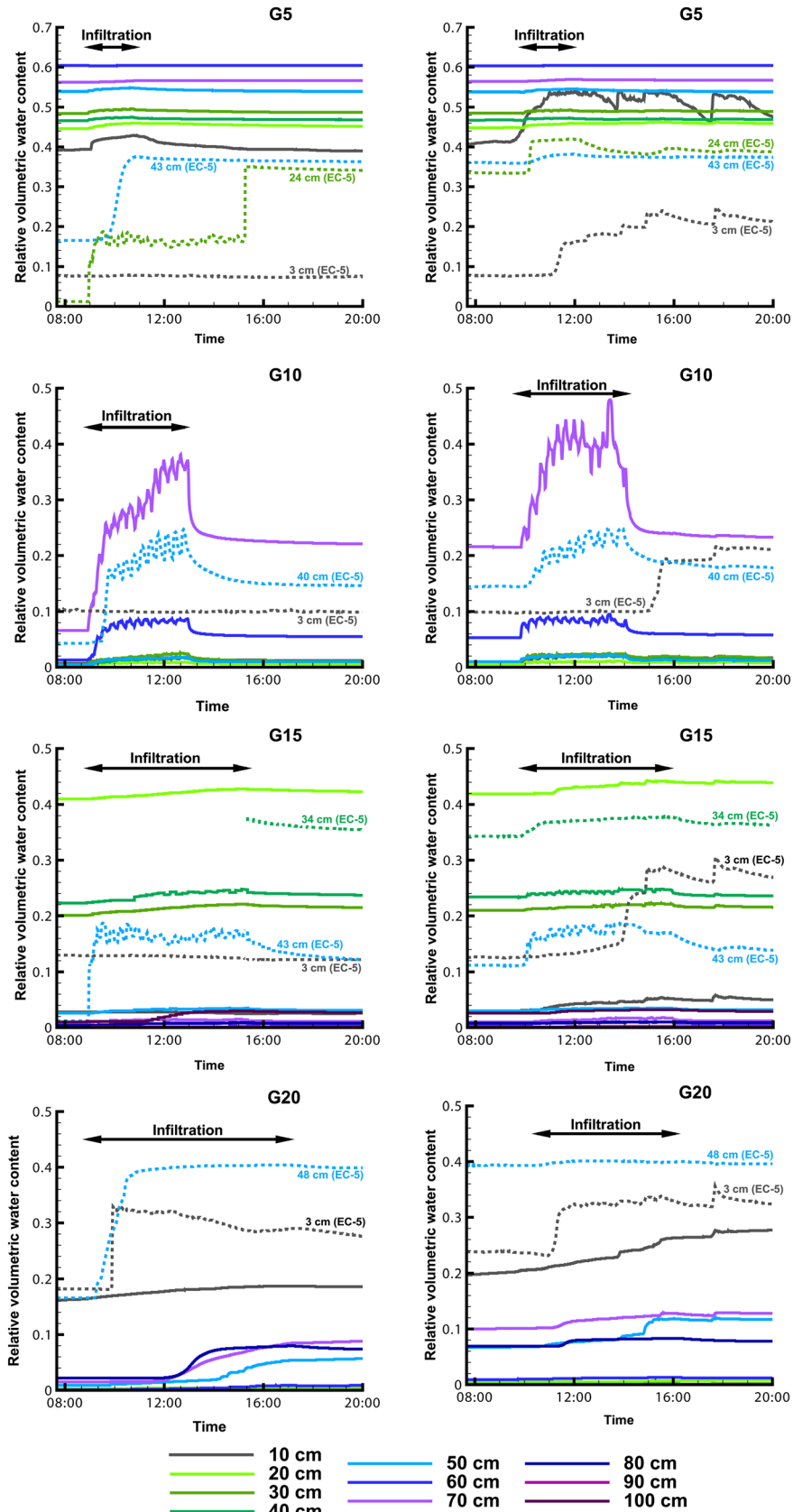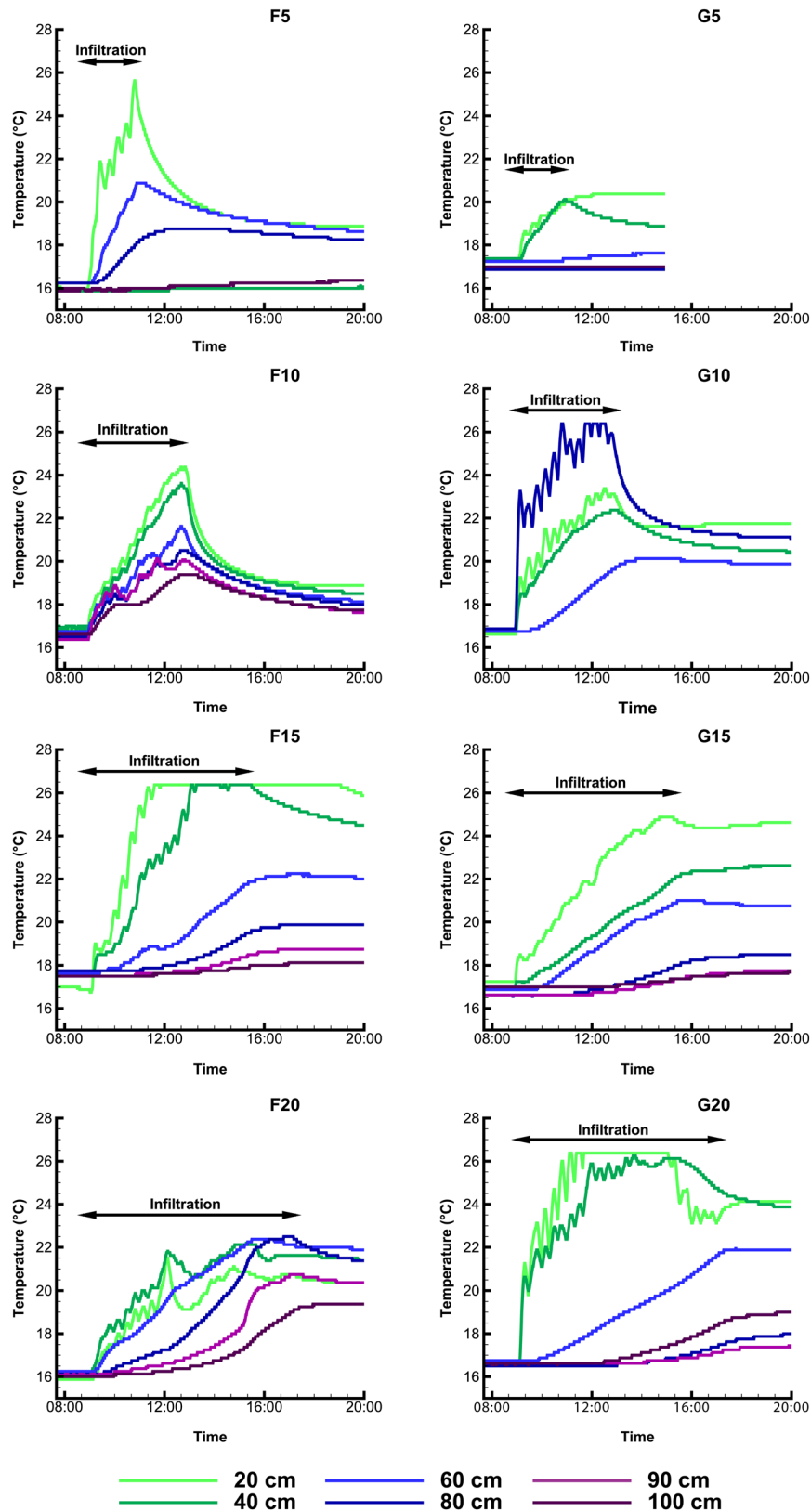
Figure 7. Continued

Figure 8. Response to the 18 September 2012 artificial infiltration event of temperature sensors. Graphs are ordered in increasing magnitude of treatment (5·1 cm at the top to 20·3 cm at the bottom). Response at different depths is indicated by different-coloured lines. Temperature rod sensors were installed at 20–100-cm depth, as indicated in the legend. Sites G5 and G10 have sensor depths that are offset from the legend (Table III). The period of infiltration at each plot is marked with a horizontal line.

Table IV. Nature of the water content and temperature sensor responses.

| Site	Water content response	Temperature response
F5	Normal progression of wetting, larger responses at greater depths	Responses at 60, and 80 prior to 40 cm with very minor responses at 40 and 100 cm
F10	Response at 75 cm prior to 65 cm	Responses at 60, 80, and 90 cm prior to 40 cm
F15	Responses at 20, 30, and 40 cm prior to 10 cm	Response at 90 cm prior to 80 cm
F20	Normal progression of wetting, larger responses at greater depths	Response at 40 cm prior to 20 cm
G5	Responses at 25, 35, and 45 cm prior to 5 and 15 cm	Normal progression of wetting with slow wetting front arrival below 50 cm
G10	Responses at 3, 23, 53, and 63 cm prior to 13, 33, and 43 cm	Responses at 33, 53, and 73 cm prior to 63 cm
G15	Responses at 26, 36, 66, and 76 cm prior to 16 and 56 cm	Normal progression of wetting with slow wetting front below 40 cm
G20	Responses at 48 and 68 cm prior to 58 cm	Response at 100 cm before 80 and 90 cm
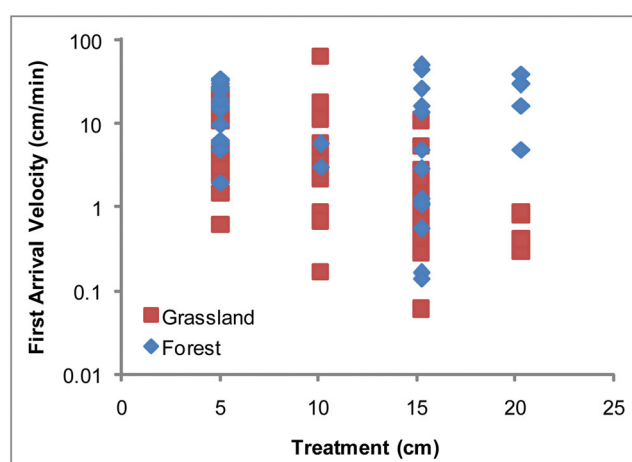
Figure 9. Measured first-arrival velocity at each sensor separated by the four irrigation treatments, simulating 5, 10, 15, and 20 cm precipitation events.

Table V. Median first-arrival velocity (cm/min) in forest and grassland plots comparing sensors at depths 1–24, 25–49, 50–74, and 75–100 cm.

Depth of sensors	Median first arrival velocity (cm/min)		P-value
	Forest	Grassland	
0–24 cm	2·5 ($n = 20$)	1·0 ($n = 12$)	0·29
25–49 cm	7·0 ($n = 12$)	3·9 ($n = 27$)	0·021*
50–74 cm	5·0 ($n = 22$)	1·2 ($n = 22$)	0·016*
75–100 cm	6·1 ($n = 26$)	0·46 ($n = 14$)	0·000013***

First arrival data is used from all four forest sites and all four grassland sites from both days of the sprinkling experiment ('dry' application and 'wet' application). First-arrival velocity is calculated using both water content and temperature sensors. *P*-values are calculated using Wilcoxon rank sum test.
*indicates *p*-value significant at 95% confidence level
***indicates *p*-value significant at 99·9% confidence level

the 2 days during which water was applied (upper graph), and water content decreases exclusive of increases for the same period (lower graph). The magnitude of the cumulative step increases of water content is greater on average in the forest than the grassland. For sensors in the 50–100-cm depth range, this forest/grassland difference is significant at the 85% confidence level. For both vegetation types, this cumulative increase also showed pronounced depth dependence, with greater water content increase for 50–100 cm than for the 0–50-cm depth interval. Cumulative step decreases showed analogous trends: greater magnitude of decrease for forest than grass, and for deeper sensors than shallower sensors.

Tests conducted at the surface and at 25-cm depth show that the grass plots have lower hydrophobicity than the forest plots. The surface hydrophobicity for grass plots ranges from 5 to 7 on the scale of Doerr (1998), with an average value of 6 (very strongly hydrophobic), whereas the forest plots range from 5 to 8 with an average of 7 (extremely hydrophobic). At 25-cm depth, the difference is more pronounced; grass plots range from 1 to 3 with an average value of 2 (hydrophilic) and forest plots range from 3 to 7 with an average of 5 (strongly hydrophobic).

DISCUSSION

Causes of observed behaviour

The ability of the forest soils to move water rapidly to depth may be attributed in part to deeper rooting of forest plants. Besides the well-known effect of macropore creation by the physical presence of roots, there is likely an accompanying increase in hydrophobicity as roots produce residues and exudates that include hydrophobic substances (Doerr, 1998). These residues and exudates, along with microbial mucilages and the cycle of wetting and drying processes, have also been found to increase soil structural complexity in the vicinity of roots, likely creating additional preferential flow paths (Czarnes *et al.*, 2000).

The greater hydrophobicity in forested areas may facilitate greater and faster downward flow. Soil with the predominant character of hydrophobicity can cause instability and preferential flow in fingers (Hardie *et al.*,
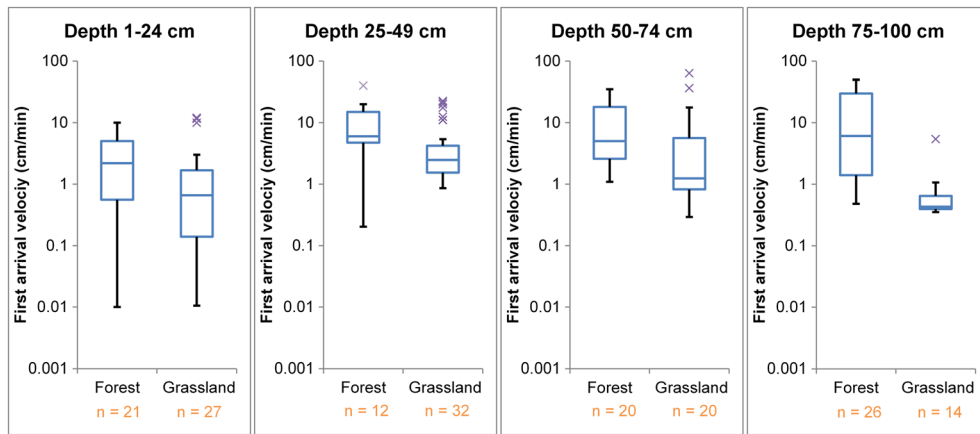
Figure 10. Cumulative increase (top) and decrease (bottom) of average volumetric water content % (VWC) over the two artificial infiltration events, 18 September 2012 and 19 September 2012. Forest data are indicated by solid lines and Grassland data are indicated by dashed lines.

2012; Xiong *et al*., 2012). This effect may be enhanced by layer contrasts in degree of hydrophobicity, and by layer-contrasts of soil hydraulic properties (Morales *et al*., 2010). Areal heterogeneities of hydrophobicity may cause small-scale lateral flow that enhances the likelihood that infiltrated water will exploit vertical preferential flow paths.

The magnitude of change and retention also varies. More water accumulated deeper in forest than grassland soil, but more was lost as well (Figure 11). There are at least two possible scenarios for this loss: water is moving rapidly enough in the forest that it is lost to deep percolation (especially at depths where root water uptake may be reduced compared with shallower depths) or (perhaps less likely because of the short times involved) plants are quickly using it for transpiration from depths >75 cm.

Limitations

We attribute differences in hydrological measurements between the two sites to the effects of restoration. However, it is possible that differing values between grasslands and restored sites may reflect spatial gradients in intrinsic soil and hydraulic properties. Based on observation, however, both forest and grassland sites had similar substrates and soil characteristics (i.e. texture and structure).

Implications

Preferential flow paths are likely more prevalent and efficient in forest soil and likely extend deeper concurrent with root depths with a relevant and important implication that forest restoration may have the potential to increase deep percolation. More water may become available for recharge as it rapidly moves to the deep unsaturated zone below the root zone, where it becomes inaccessible to plants. Brauman *et al*. (2012a) studied the effects of land cover on recharge on the island of Hawai'i and found that for the majority of rainstorms, water moves quickly below

rooting depths thereby limiting evapotranspiration. However, rainfall is twice as great at the location Brauman investigated (1500–2000 mm annually) than it is at Auwahi (average 730 mm annually).

Some studies of restoration, with non-native tree species, showed no potential to increase deep percolation and recharge (Restom-Gaskill, 2004; Little *et al*., 2009). At the Honouliuli Preserve on the island of Oahu, fast-growing non-native species (eucalyptus) were planted in the early 1900s to reduce erosion and hydrologic impacts caused by grazing and native tree (*Acacia koa*) extraction in the 1800s. Restom-Gaskill (2004) found that the eucalyptus planted at Honouliuli used more water than native species, thereby allowing less recharge.

Previous isotopic studies give us insight into water use of native species such as *olopua* (*N. sandwicensis*). Stratton *et al*. (2000) used stable hydrogen isotopes to examine rooting depths of several species on the island of Lana'i including *olopua*. They found that *olopua*, though it may have deeper roots than invasive grasses, primarily drew water from the upper portion of the soil profile (20–30-cm depth) in order to exploit light precipitation events. Cordell and Sandquist (2008) evaluated the impact of the invasive fountain grass (*Pennisetum setaceum*) on the native tree *Diospyros sandwicensis* resource acquisition on the island of Hawai'i using stable oxygen isotopes. They found that trees growing within fountain grass stands had less root activity in the top 20 cm of the soil column that was dominated by fountain grass roots compared with trees growing in an adjacent area where fountain grass had been removed. It is possible that a similar water-use relationship exists at the Auwahi site. Brauman *et al*. (2012b) found that in Kona, Hawai'i, kikuyu grasslands have the potential to transpire just as much or even more than the adjacent dry forests, given little or no water stress.

Our experiment provides valuable insights into comparative water flow behaviour between forest and grassland
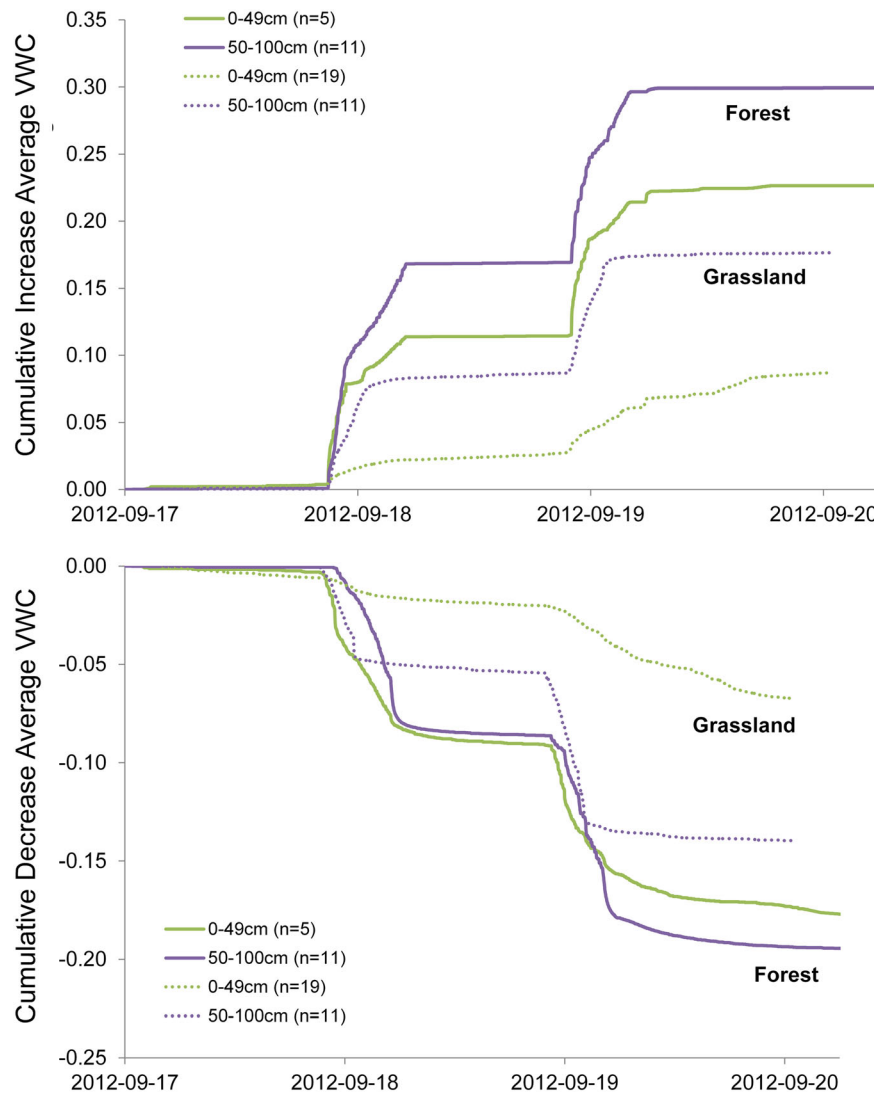
Figure 11. Difference in first-arrival velocities between forest and grassland locations. Box-and-whisker plot comparisons of four depth classifications: 0–24-, 25–49-, 50–74-, and 75–100-cm depth. The box indicates the data in the second and third quartiles, with the line in the middle of the box indicating the median. The top whisker indicates the spread of data in the fourth quartile and the bottom whisker indicates the spread of data in the first quartile. Outliers (values greater than 1·5 times the interquartile range above the third quartile or values less than 1·5 times the interquartile range below the first quartile) are indicated by the purple x's.

given equal amounts of applied precipitation. Other natural processes not accounted for in our experiments may affect total amounts of infiltrated water during natural precipitation events. Influences on soil water not accounted for during the sprinkling experiment include cloud/fog water and the interception of precipitation by canopy vegetation and groundcover/leaf litter. The Auwahi site is at the lower boundary of a cloud belt that forms from thermal air flow (sea breeze dynamics) (Scholl *et al.*, 2007). Cloud water has been found (using a water budget method) to be a significant contribution to soil water at the Auwahi site under natural conditions. Giambelluca *et al.* (2011b) found that cloud water interception within the Auwahi forest is 16·6 cm year^{-1} with 74% of that becoming throughfall. A previous isotopic study at Auwahi showed that as much as

46% of precipitation is derived from orographic cloud water (Scholl *et al.*, 2007). Thus, it is possible that because it has more canopy surface area to intercept cloud water, the forest may receive more total precipitation than the grassland. Tsiko *et al.* (2012) examined differences in precipitation interception by forest leaf litter and adjacent thatch grasses. They found that, for their study site, forest leaf litter had 4% more precipitation storage capacity than the grasses. They also noted a storm size threshold (larger storm intensity results in decreased storage capacity). If the same relationship exists at Auwahi, it might be expected that the grassland would have slightly more subsurface soil moisture than the forest. The competing effects of canopy interception, increased moisture from fog water in the forest, and interception of water by ground cover are difficult to

quantify based on our experiments. Instrumentation installed for this study will remain in place for at least 1 year to monitor subsurface responses to natural water inputs of rainfall and cloud/fog water. Additionally, plant monitoring with sap flow sensors will contribute to understand how transpiration from vegetation affects soil moisture and potential recharge.

The pronounced differences in soil–water behaviour that result from a 15-year forest restoration project reinforce and broaden conclusions of our earlier ecohydrologic study at the Auwahi site (Perkins *et al.*, 2012). Soil development, specifically concerning properties affecting water movement and retention, is an important element of the changes effected by forest restoration. The changes in soil which occur during the transition from one land use type to another, in large part advanced by the plants themselves, are a vital component of restoration or reestablishment of native ecosystems.

SUMMARY

Land-use changes profoundly impact unsaturated-zone biotic and hydrologic processes including subsurface moisture dynamics. Soil recovery with landscape change is a major ecohydrologic influence. The Auwahi forest restoration project (www.auwahi.org) provides a setting for comparing the hydrology of native forest and invasive grassland. Restoration with native species at the Auwahi site has significantly altered the hydrology of the unsaturated zone to at least 1-m depth. During infiltration at grassland sites, water movement slowed with depth, whereas, at reforested sites, water movement was rapid through the entire uppermost metre of soil. Reforested areas appear to facilitate deep water transfer relative to grassland sites. Though small in scale, this experiment provides strong inferential evidence of the profound role that forest soil structure has in contributing to deep soil percolation in high-rainfall events. Interestingly, the total amount of irrigated water did not appear to correlate with first water arrival velocities or magnitudes of water content change. Data and observations from this study along with inferences from other studies suggest that restoration projects such as Auwahi can have significant ecohydrologic effects, such as promoting more rapid deep movement of water and potentially increasing the amount of soil water available for recharge.

ACKNOWLEDGEMENTS

REFERENCES

Alaoui A, Caduff U, Gerke H, Weingartner R. 2011. Preferential flow effects on infiltration and runoff in grassland and forest soils. *Vadose Zone Journal* **10**(1): 367–377.

Bachmair S, Weiler M, Nützmann G. 2009. Controls of land use and soil structure on water movement: lessons for pollutant transfer through the unsaturated zone. *Journal of Hydrology* **369**(3): 241–252.

Berglund ER, Ahyoud A, Tayaa MH. 1980. Comparison of soil and infiltration properties of range and afforested sites in northern Morocco. *Forest Ecology and Management* **3**: 295–306.

Brauman KA, Fryberg DL, Daily GC. 2012a.Land cover effects on groundwater recharge in the tropics: ecohydrologic mechanisms. *Ecohydrology* **5**: 435–444.

Brauman KA, Freyberg DL, Daily GC. 2012b. Potential evapotranspiration from forest and pasture in the tropics: a case study in Kona, Hawai'i. *Journal of Hydrology* **440–441**: 52–61.

Cabin RJ, Weller SG, Lorence DH, Flynn TW, Sakai AK, Sandquist D, Hadway LJ. 2001. Effects of long-term ungulate exclusion and recent alien species control on the preservation and restoration of a Hawaiian tropical dry forest. *Conservation Biology* **14**(2): 439–453.

Cordell S, Sandquist D. 2008. The impact of an invasive African bunchgrass (*Pennisetum setaceum*) on water availability and productivity of canopy trees within a tropical dry forest in Hawaii. *Functional Ecology* **22**(6): 1008–1017.

Czarnes S, Hallett P, Bengough A, Young I. 2000. Root- and microbial-derived mucilages affect soil structure and water transport. *European Journal of Soil Science* **51**(3): 435–443.

D'Odorico P, Caylor K, Okin GS, Scanlon TM. 2007. On soil moisture-vegetation feedbacks and their possible effects on the dynamics of dryland ecosystems. *Journal of Geophysical Research* **112**: G04010.

Doerr SH. 1998. On standardizing the 'Water Drop Penetration Time'and the 'Molarity of an Ethanol Droplet'techniques to classify soil hydrophobicity: a case study using medium textured soils. *Earth Surface Processes and Landforms* **23**(7): 663–668.

Gee GW, Or D. 2002. Particle size analysis. In *Methods of Soil Analysis, Part 4—Physical Methods, Soil Sci. Soc. Am. Book Ser.*, vol. **5**, Dane J. H., Topp G. C. (eds). Soil Sci. Soc. of Am.: Madison, Wis; pp. 255–293.

Giambelluca TW, Chen Q, Frazier AG, Price JP, Chen Y-L, Chu P-S, Eischeid J, Delparte D. 2011a. The Rainfall Atlas of Hawai'i. http://rainfall.geography.hawaii.edu.

Giambelluca TW, DeLay JK, Nullet MA, Scholl MA, Gingerich SB. 2011b. Canopy water balance of windward and leeward Hawaiian cloud forests on Haleakalā, Maui, Hawai'i. *Hydrological Processes* **25**(3): 438–447.

Gingerich, SB. 2008. Ground-water availability in the Wailuku area, Maui, Hawaii. *USGS SIR* 2008-5236.

Godsey S, Elsenbeer H. 2002. The soil hydrologic response to forest regrowth: a case study from southwestern Amazonia. *Hydrological Processes* **16**(7): 1519–1522.

Grayson RB, Western A, Walker J, Kandel D, Costelloe J, Wilson D. 2006. Controls on patterns of soil moisture in arid and semi-arid systems. In *Dryland Ecohydrology*, D'Odorico P, Porporato A (eds.). Springer; 109–127.

Hardie M, Deurer M, Doyle RB, Lisson S, Cotching WE, Mattern K. 2012. Development of unstable flow and reduced hydraulic conductivity due to water repellence and restricted drainage. *Vadose Zone Journal* **11**(4). DOI: 10.2136/vzj2011.0099.

Ilstedt U, Malmer A, Verbeeten E, Murdiyarso D. 2007. The effect of afforestation on water infiltration in the tropics: a systematic review and meta-analysis. *Forest Ecology and Management* **251**(1): 45–51.

Little C, Lara A, McPhee J, Urrutia R. 2009. Revealing the impact of forest exotic plantations on water yield in large scale watershed in South-Central Chile. *Journal of Hydrology* **374**: 162–170.

Medeiros AC, von Allmen E. 2006. Restoration of native Hawaiian dryland forest at Auwahi, Maui. *USGS Fact Sheet* **2006-3035**.

Medeiros AC, Loope LL, Holt RA. 1986. Status of native flowering plant species on the south slope of Haleakala, East Maui, Hawaii. Honolulu (HI): Cooperative National Park Resources Studies Unit, University of Hawaii at Manoa, Department of Botany. *PCSU Technical Report 59*.

Medeiros AC, Davenport C, Chimera CG. 1998. Auwahi: ethnobotany of a dryland forest. Cooperative National Park Resources Studies Unit, University of Hawaii at Manoa, Department of Botany. *PCSU Technical Report 117*.

Medeiros AC, Erwin TL, CG Chimera, LL Loope. 2003. Vegetation trends at auwahi dryland forest after five years of restoration (hawaii). *Ecological Restoration* **21**(3): 207–209.

Medeiros AC, vonAllmen E, Chimera CG. 2013. Dry forest restoration and unassisted native tree seedling recruitment at Auwahi, Maui, 1997-2012. *Pacific Science* **68**(1): 25 pp.

Morales VL, Parlange J-Y, Steenhuis TS. 2010. Are preferential flow paths perpetuated by microbial activity in the soil matrix? A review. *Journal of Hydrology* **393**: 29–36.

Nimmo JR, Perkins KS, Schmidt KM, Miller DM, Stock JD, Singha K. 2009. Hydrologic characterization of desert soils with varying degrees of pedogenesis: 1. Field experiments evaluating plant-relevant soil water behavior. *Vadose Zone Journal* **8**(2): 480–495.

Perkins K, Nimmo J, Medeiros A. 2012. Effects of native forest restoration on soil hydraulic properties, Auwahi, Maui, Hawaiian Islands. *Geophysical Research Letters* **39**(5): L05405.

Restom-Gaskill TG. 2004. Hydrology of forest ecosystems in the Honouliuli Preserve: implications for groundwater recharge and watershed restoration. University of Hawaii at Manoa, Honolulu, Hawaii, USA. PhD Dissertation.

Rock JF. 1913. *The Indigenous Trees of the Hawaiian Islands*. J.F. Rock Press: Honolulu.

Sandvig RM, Phillips FM. 2006. Ecohydrological controls on soil moisture fluxes in arid to semiarid vadose zones. *Water Resources Research* **42**(8): W08422.

Scholl M, Giambelluca T, Gingerich S, Nullet M, Loope L. 2007. Cloud water in windward and leeward mountain forests: the stable isotope signature of orographic cloud water. *Water Resources Research* **43**(12): W12411.

Stewart-Deaker AE, Moore SJ, Stonestrom DA. 2007. Streamflow, infiltration, and ground-water recharge at Abo Arroyo, New Mexico. *US Geological Survey Professional Paper* **1703**: 83–106.

Stock J, Coil J, Kirch PV. 2003. Paleohydrology of arid southeastern Maui, Hawaiian Islands, and its implications for prehistoric human settlement. *Quaternary Research* **59**(1): 12–24.

Stratton LC, Goldstein G, Meinzer FC. 2000. Temporal and spatial partitioning of water resources among eight woody species in a Hawaiian dry forest. *Oecologia* **124**(3): 309–317.

Tsiko, CT, Makurira, H, Gerrits, AMJ, Saveniji, HHG. 2012. Measuring forest floor and canopy interception in a savannah ecosystem. *Recent Advances in Water Resources Management.* **47-48**: 122–127.

USDA Soil Survey Division Staff. 1993. Soil survey manual. Soil Conservation Service. *U.S. Department of Agriculture Handbook* 18.

USDA Soil Survey Division Staff. 2001. Ulupalakua series. https://soilseries.sc.egov.usda.gov/OSD_Docs/U/ULUPALAKUA.html. Accessed 12/19/2013

Wahren A, Feger K-H, Schwärzel K, Münch A. 2009. Land-use effects on flood generation-considering soil hydraulic measurements in modelling. *Advances in Geosciences* **21**: 99–107.

Xiong Y, Furman A, Wallach R. 2012. Moment analysis description of wetting and redistribution plumes in wettable and water-repellent soils. *Journal of Hydrology* **422-423**: 30–42.

Zar JH. 1999. *Biostatistcal Analysis*, 4th edn. Prentice Hall: Upper Saddle River, New Jersey. 663 pp.

Zhou X, Lin H, White E. 2008. Surface soil hydraulic properties in four soil series under different land uses and their temporal changes. *Catena* **73**(2): 180–188.

Zimmermann B, Elsenbeer H. 2008. Spatial and temporal variability of soil saturated hydraulic conductivity in gradients of disturbance. *Journal of Hydrology* **361**(1): 78–95.